Dossier

This paper is a part of the hereunder thematic dossier published in OGST Journal, Vol. 69, No. 5, pp. 773-969 and available online here

Cet article fait partie du dossier thématique ci-dessous publié dans la revue OGST, Vol. 69, n°5, pp. 773-969 et téléchargeable ici

DOSSIER Edited by/Sous la direction de : **P.-L. Carrette**

PART 1
Post Combustion CO_2 Capture
Captage de CO_2 en postcombustion

Oil & Gas Science and Technology – Rev. IFP Energies nouvelles, Vol. 69 (2014), No. 5, pp. 773-969

Oil & Gas Science and Technology – Rev. IFP Energies nouvelles, Vol. 69 (2014), No. 5, pp. 851-864

DOI: 10.2516/ogst/2013155

Dossier

Post Combustion CO_2 Capture
Captage de CO_2 en postcombustion

CO_2 Absorption by Biphasic Solvents: Comparison with Lower Phase Alone

Zhicheng Xu, Shujuan Wang*, Guojie Qi, Jinzhao Liu, Bo Zhao and Changhe Chen

Key Laboratory for Thermal Science and Power Engineering of Ministry of Education, Beijing Key Laboratory for CO_2 Utilization and Reduction Technology, Department of Thermal Engineering, Tsinghua University, Beijing 100084 - China
e-mail: wangshuj@tsinghua.edu.cn

* Corresponding author

Résumé — Absorption du CO_2 par des solvants biphasiques : comparaison avec la phase inférieure isolée — Il a été montré que les mélanges de 1,4-butanediamine (BDA) 2 M et 2-(diéthylamino)-éthanol (DEEA) 4 M sont des solvants biphasiques prometteurs. Dans cette étude la composition de la phase inférieure est déterminée en utilisant un chromatographe ionique (CI) DX-1290 et un titrateur automatique *Metrohm* 909 Titrando. Les capacités cycliques, les taux de charge cycliques et les produits de réaction du solvant biphasique sont comparés à ceux d'une solution aqueuse de même concentration en amines que la phase inférieure du solvant biphasique au taux de charge riche ($(2B4D)_L$), en utilisant des équipements de screening rapide et un spectromètre à Résonance Magnétique Nucléaire (RMN) JNM ECA-600. Les vitesses d'absorption ont aussi été mesurées à différents taux de charge sur film tombant. Les résultats indiquent que la capacité cyclique et le taux de charge cyclique de $(2B4D)_L$ sont très proches de celles de 2B4D. La vitesse d'absorption de $(2B4D)_L$ est plus élevée que celle de 2B4D pour les trois taux de charge étudiés, sauf dans le cas d'une solution vierge à une pression partielle de CO_2 inférieure à 10 kPa. Les résultats de RMN indiquent que les produits de réaction de $(2B4D)_L$ comportent plus de bicarbamate de BDA, moins de BDA et moins de carbamate de BDA que 2B4D. Les produits de réaction de $(2B4D)_L$ avec le CO_2 comportent deux fois plus de carbonate/bicarbonate que dans le cas de 2B4D et moins de carbamate de BDA.

Abstract* — *CO_2 Absorption by Biphasic Solvents: Comparison with Lower Phase Alone — *The mixtures of 2 M 1,4-butanediamine (BDA) and 4 M 2-(diethylamino)-ethanol (DEEA) have been found to be promising biphasic solvents. This work identifies the composition of the lower phase using a DX-120 Ion Chromatograph (IC) and a* Metrohm *809 Titrando auto titrator. The cyclic capacities, cyclic loadings and reaction products of the biphasic solvent are compared with those of the aqueous solution with the same amine concentration as the lower phase of the biphasic solvent at the rich loading ($(2B4D)_L$) using a fast screening facility and a JNM ECA-600 Nuclear Magnetic Resonance spectrometer (NMR). Their absorption rates at different loadings are also investigated using a Wetted Wall Column (WWC). The results show that the cyclic capacity and cyclic loading of $(2B4D)_L$ are almost the same as those of 2B4D. The absorption rate of $(2B4D)_L$ is higher than 2B4D at all the 3 tested loadings, except for the fresh solutions at CO_2 pressure lower than 10 kPa. NMR results show that the reaction products of $(2B4D)_L$ had more BDA bicarbamate, less BDA and less BDA carbamate than 2B4D. The CO_2 reaction products of $(2B4D)_L$ had twice as much carbonate/bicarbonate as with 2B4D and less BDA carbamate.*

INTRODUCTION

Over the last decades, amine gas sweetening has become a proven technology for the CO_2 capture from natural gas. In recent years, amine based absorption has also been widely investigated for CO_2 capture in power plant, due to its high flexibility and easy retrofit for existing power plant (Rochelle, 2009). Development of solvents with high efficiency is regarded as one of the most crucial issues for CO_2 absorption. Many solvents, such as monoethanolamine (MEA), methyldiethanolamine (MDEA), diethanolamine (DEA) and piperazine (PZ), have been applied to capture CO_2 (Bishnoi and Rochelle, 2002; Derks and Dijkstra, 2005; Rinker *et al.*, 2000; Rinker and Ashour, 2000). However, this absorption-desorption process always requires lots of energy and high operation costs during solvent regeneration. Therefore, to minimize the energy penalty is of great importance for this absorption-desorption system.

Recent years, some novel concepts, such as DMX^{TM} (Raynal *et al.*, 2011) and lipophilic amine solvents (Zhang X., 2007), have been proposed for the improvement of the energy performance. Zhang J. *et al.* (2011) did screening tests of dipropylamine (DPA), dimethylcyclohexylamine (DMCA) and other solvents. Tan (2010) studied the kinetics and thermodynamics of DPA and DMCA blend and found that the cyclic loading of this solvent can reach 0.7 mol CO_2/mol amine. The precipitation of the solvent at high loading, however, is still a challenge for this system. Raynal *et al.* (2011) explained the DMX^{TM} process, which, according to their simulations, could remarkably reduce the reboiler heat duty to 2.3 GJ/t CO_2. Rojey *et al.* (2009) found that some solvents with special structures can separate into two liquid phases after absorption, but they did not give the particular structures. Hu (2009) pointed out that biphasic solvents should consist of several compounds, including at least one activator A and one solvent B, and that the mixture composition should be 20% A plus 80% B. However, Hu (2009) did not give the exact amines in the solvents. Bruder and Svendsen (2011) found that a blend of 5 M DEEA and 2 M MAPA separated into two phases after CO_2 absorption, with a cyclic loading higher than that of 5 M MEA. The lower phase, however, was found to be viscous, which affected the transition of the lower phase to the stripper.

Cyclic capacity ΔR, expressed as either C_{amine} $(\alpha_{rich} - \alpha_{lean})$ or $R_{abs}-R_{des}$, is an important characteristic of the solvent, where C_{amine} is the amine concentration, R_{abs} and R_{des} are the CO_2 concentrations in terms of moles per kilogram after absorption and desorption; α_{rich} and α_{lean} are rich and lean loading of the solvent, the difference of which is shown as cyclic loading, $\Delta\alpha$. Cyclic efficiency, θ, is the result of $\Delta\alpha$ divided by α_{rich}. A promising solvent should have relatively higher cyclic capacity, cyclic loading and cyclic efficiency (Aronu *et al.*, 2011).

About 30 solvents with various compositions, including solutions with Low Critical Solution Temperature (LCST) and other potential biphasic solvents, were screened in our previous research (Xu *et al.*, 2012a,b, 2013a,b,c). Some of these biphasic solvents, such as 5 M TEA and 2 M BDA blended with 4 M DEEA, have been proven to have higher cyclic capacities, cyclic loadings or absorption rates than traditional 5 M MEA. Moreover, the aqueous solution of 2 M BDA mixed with 4 M DEEA (simplified as 2B4D hereafter) was found to have the best performance among the selected solvents, with 46% higher cyclic loading, 48% higher cyclic capacity and 11% higher cyclic efficiency than 5 M MEA, which will reduce the sensible heat requirement during regeneration (Svendsen *et al.*, 2011).

It was found that the solution of 2B4D became two phases after CO_2 absorption using the fast screening facility on the absorption mode, with 97.4% of CO_2 existing in the lower phase and a total loading of 0.505 mol CO_2/mol amine. The weight percentages of the upper and lower phases after absorption on the absorption mode were 21.79% and 78.21%, respectively. The screening facility will be described in the experimental section. The amine and CO_2 distributions in the two phases were analyzed by IC in the previous studies. It was confirmed that the biphasic solvent separation is due to the fast reaction rate of BDA with CO_2 and the limited solubility of DEEA in the reaction products of BDA with CO_2. The reaction products of BDA in the two phases were then analyzed. The products was mainly BDA carbamate in the upper phase, while in the lower phase, at a total loading of 0.446 mol/mol amine, the mole fractions of BDA, BDA carbamate and BDA bicarbamate were 16.8%, 55.8% and 27.4% respectively (Xu *et al.*, 2013c). Since most of the CO_2 absorbed existed in the lower phase after absorption, comparison of the alone lower phase and biphasic solvent is necessary to decide which one will be more efficient.

This paper will identify the composition of 2B4D lower phase after absorption. Then, the absorption and desorption properties of the alone lower phase of 2B4D (simplified as $(2B4D)_L$ hereafter), which has the same amine concentration as the 2B4D lower phase at rich loading, will be measured and compared with 2B4D. The absorption rates of 2B4D and $(2B4D)_L$ at different loadings will be compared with WWC. The reaction products of $(2B4D)_L$ with CO_2 during absorption will also be measured by NMR and compared with those of 2B4D.

1 EXPERIMENTAL

The chemicals used in this work, BDA (≥98 wt%), DEEA (≥99 wt%), dioxane (≥99.5 wt%) and D_2O (≥99.96 wt%) NaOH (≥96 wt%) from *Aladdin Reagent Company*, and CO_2 (≥99.9% pure), SO_2 (1.51% vol%, N_2 balanced) and N_2 (≥99.99% pure) from *Beijing Huayuan Gas Company* were used without further purification. Distilled deionized water was used for preparing the solutions. The amine concentrations were determined by titration against 0.2 N H_2SO_4 using a *Metrohm* 809 Titrando auto titrator.

The BDA and DEEA structures are shown Figure 1.

The absorption and desorption capacities, and the rich and lean loadings were measured using a fast screening facility, and the loadings were confirmed by the titration method. The absorption experiments were conducted at 40°C with the desorption at 90°C at atmospheric pressure. On "absorption mode", CO_2 and N_2, controlled by mass flow controller, were used to simulate the flue gas with 12% of CO_2 in terms of volume. The total gas flow rate was 463 mL/min. The simulated flue gas went through the gas mixture first to mix intensively, and then to the reactor, which was made of glass and had a volume of about 150 mL. After reaction with solvent, the gas went to condenser, which was circulated by 3°C water. The condensed water went back to the reactor to avoid water losses, and then the acid washing, in case that amine vapor mixed with simulated gas and resulted in measurement error in IR CO_2 analyzer. After being dried by anhydrous calcium chloride, CO_2 concentration of the gas was measured by the IR CO_2 analyzer. Equilibrium was assumed to be reached when the outlet CO_2 concentration reached 12%. On "desorption mode", N_2 was used to sweep the desorbed CO_2 to take turns in going through condenser, acid washing, drier and analyzer with a flow rate of 874 mL/min. Lean loading of solution was assumed to be reached when the outlet CO_2 concentration was less than 0.1%. This assumption has been verified in our previous work (Xu *et al.*, 2012a). The volume of the fresh solution added in the reactor was 100 mL. The other details of the facility were described by Xu *et al.* (2012a).

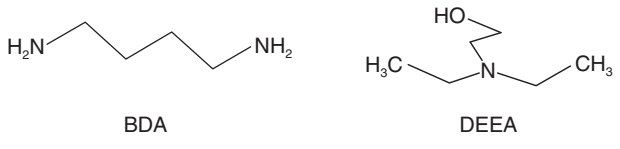

Figure 1
BDA and DEEA structures.

A wetted wall column was used to investigate the absorption rate of the amine solution with a contact area of about 41.45 cm^2. The gas-liquid contactor was constructed from a stainless steel tube, measuring 11.0 cm in height and 1.2 cm in diameter. The gas-liquid contact region was enclosed by a 31.0 cm thick-walled glass tube, separated from a water bath. More details about the original WWC system can be found in our previous research (Liu *et al.*, 2009, 2011, 2012). The experimental system used in this work shown in Figure 2 has two modifications from the original system. A saturator with the same temperature and pressure as the reactor was added before the gas entered the reactor. The gas side mass transfer coefficient was calibrated using SO_2 absorption into NaOH solution, to replace the previous one which was determined with CO_2 absorption into MEA solution.

For the analysis method, A *Dionex* DX-120 system with an IonPac Column CG17/CS17 was used to measure the individual amine concentrations in the two liquid phases. The CO_2 loading was determined by titration using the barium carbonate precipitation method (Hilliard, 2008). A JNM ECA-600 NMR from *JEOL Company* was used to analyze the reaction products in the solution in terms of ^{13}C. As the natural abundance of ^{13}C is 1.11%, the ordinary CO_2 was added into the solution for further analysis. CO_2 was added by bubbling the gas into the solution. The total loading was determined from the weight change of the solution after bubbling with CO_2, and the individual loadings of the upper and lower phases were titrated. Then, about 1 mL solution was added to a WG-5000-7-50 sample tube from *Wilmad Company*. Dioxane was used as an internal standard and a small amount of D_2O was added to the sample tube to get a signal lock. The magnetic field strength of the NMR was 14.096 T, with a ^{13}C resonance frequency of 150.91 MHz. The quantitative ^{13}C lasted 15 hours for each sample with a relaxation time of 20 seconds.

2 THEORY

2.1 Chemical Reactions

The chemical reactions of CO_2 with the amines in the solution can be addressed as follows:

Dissociation of carbon dioxide:

$$CO_2 + 2H_2O \leftrightarrow HCO_3^- + H_3O^+ \quad (1)$$

Dissociation of bicarbonate ion:

$$HCO_3^- + H_2O \leftrightarrow CO_3^{2-} + H_3O^+ \quad (2)$$

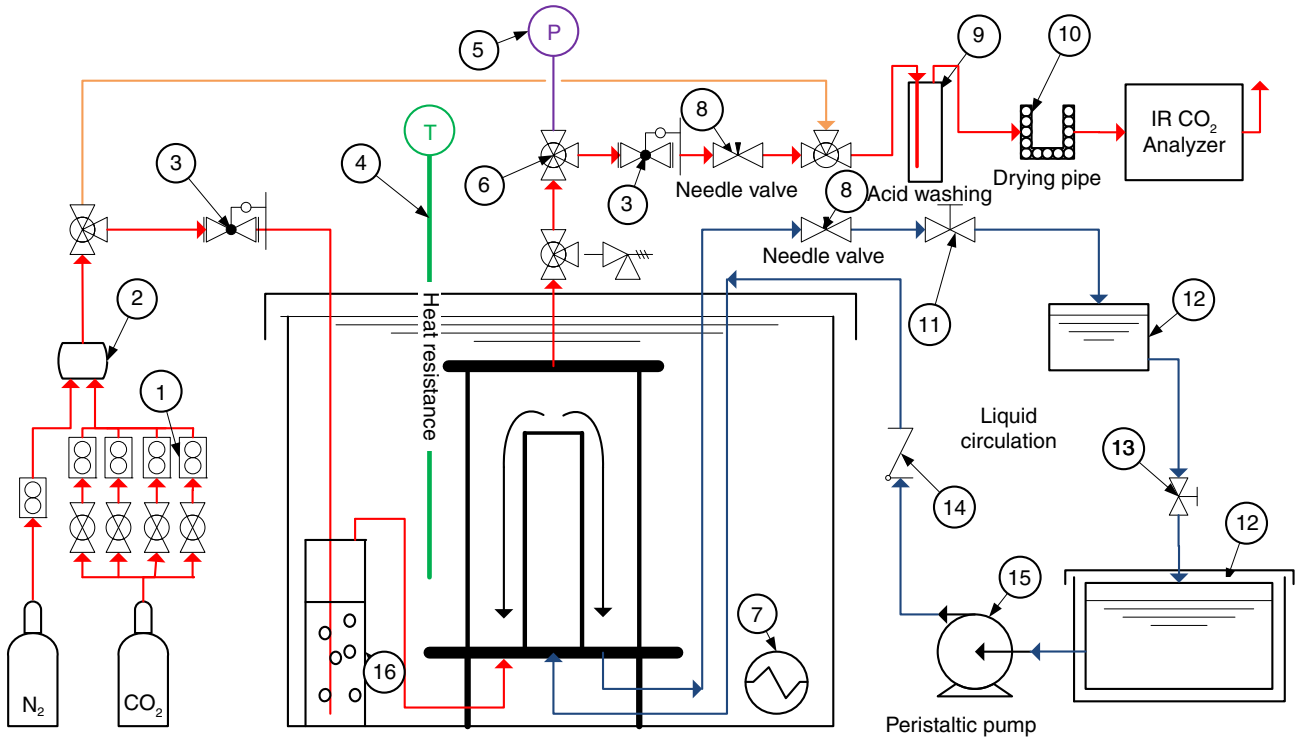

1. Mass flow controller 2. Cylinders mixed 3. Gas valves 4. Heat resistance heater 5. Pressure transmitter 6. Three-way valve 7. Electric heater 8. Precision needle valve 9. Acid wash 10. Drying pipe 11. Liquid valves 12. Liquid storage tank 13. Rotary screw valve 14. One-way valve 15. High-pressure peristaltic pump 16. Saturator

Figure 2
The experiment scheme of wetted wall column.

Dissociation of protonated amine:

$$DEEAH^+ + H_2O \leftrightarrow DEEA + H_3O^+ \quad (3)$$

$$BDAH^+ + H_2O \leftrightarrow BDA + H_3O^+ \quad (4)$$

Dissociation of deprotonated BDA:

$$BDAH_2{}^{2+} + H_2O \leftrightarrow BDAH^+ + H_3O^+ \quad (5)$$

Formation of carbamate of BDA:

$$BDA + CO_2 + H_2O \leftrightarrow BDACOO^- + H_3O^+ \quad (6)$$

Formation of bicarbamate of BDA:

$$BDACOO^- + CO_2 + H_2O \leftrightarrow BDA(COO)_2{}^{2-} + H_3O^+ \quad (7)$$

Dissociation of protonated carbamate:

$$BDAHCOO + H_2O \leftrightarrow BDACOO^- + H_3O^+ \quad (8)$$

2.2 Absorption Rate Calculation of WWC

Based on the two film model, the mass flux with chemical absorption can be described as follows, where the total resistance to mass transfer is divided as the sum of the resistance from gas side and liquid side, as Equation (9) shows:

$$\frac{1}{k_g} + \frac{1}{k_G'} = \frac{1}{K_G} \quad (9)$$

The overall gas transfer coefficient, K_G, can be calculated from the *Flux*, $P_{CO_2,in}$ and $P_{CO_2,out}$. K_G is fixed for a given temperature and amine concentration and can be calculated by the *Flux*-CO_2 partial pressure curve:

$$K_G = \frac{Flux}{P_{CO_2,b} - P^*_{CO_2}} \quad (10)$$

where $P_{CO_2,b}$ is the operational partial pressure of CO_2 in the wetted wall column, which is the log mean average, as Equation (11) shows:

$$P_{CO_2,b} = \frac{P_{CO_2,in} - P_{CO_2,out}}{Ln(P_{CO_2,in}/P_{CO_2,out})} \quad (11)$$

The CO_2 pressure in the gas-liquid contact face, $P_{CO_2,i}$, can be calculated by Equation (12):

$$k_g = \frac{Flux}{P_{CO_2,b} - P_{CO_2,i}} \quad (12)$$

The gas side mass transfer coefficient k_g can be given by Equation (13):

$$Sh = \alpha(Re \times Sc \times d_h/h)^{\beta} \quad (13)$$

where $Sh = RTk_g d_h D_{CO_2}, Re = \rho_g V_g d_h/\mu_g$, $Sc = \upsilon/D$, d_h is the hydraulic diameter of the annulus and h is the length of the column. As Pacheco (1998) stated, the parameters α and β are fitted based on the experimental data of SO_2 absorption into 0.1 M NaOH solution. The fitted results will be presented in Section 3.3.

3 RESULTS AND DISCUSSION

3.1 $(2B4D)_L$ Identification and the Lean Loading Calculation

The amine and CO_2 concentrations in the two phases were measured by IC and auto-titrator after the CO_2 absorption by 2B4D reaching equilibrium using the fast screening facility on absorption mode. The measurement error has been evaluated in previous work and the results proven to be reliable (Xu *et al.*, 2013c). At the rich loading, the BDA, DEEA and CO_2 concentrations in the lower phase were 2.23, 2.40 and 3.29 mol/kg solution, which can be converted to the amine concentration of $(2B4D)_L$ by subtracting the weight of CO_2 in the solution. The actual BDA and DEEA concentrations in fresh $(2B4D)_L$ solution were 2.61 and 2.81 mol/kg.

The absorption rates of 2B4D and $(2B4D)_L$ at lean loadings were measured to compare their performance comprehensively. Thus, the lean loadings of 2B4D and $(2B4D)_L$ were identified here. The 2B4D lean solution was got using the fast screening facility on desorption mode and the CO_2 loading of the lean solution was titrated. The rich and lean solutions of $(2B4D)_L$ were got using the fast screening facility on absorption and desorption mode, respectively. Then the CO_2 loadings of $(2B4D)_L$ rich and lean solution were titrated using the titrator. The CO_2 and amine concentrations in 2B4D lean solution were the mixture of upper phase and the lean solution of lower phase, the same as would occur in actual application.

Table 1 presents the BDA, DEEA and CO_2 concentrations in 2B4D upper and lower phases at lean and rich CO_2 loadings, as well as those of $(2B4D)_L$ solutions at lean and rich CO_2 loadings. The amine and CO_2 concentrations are between the concentrations for the upper phase solution and the lean solution of lower phase. Table 1 reveals that the $(2B4D)_L$ lean solution has higher BDA concentration, lower DEEA concentration, slightly higher CO_2 concentration and higher CO_2 loading than 2B4D lean solution.

3.2 Comparisons of the Cyclic Capacity and Cyclic Loading

Our previous works have confirmed the reliability of the screening and titration results (Xu *et al.*, 2012a, 2013c).

TABLE 1
BDA, DEEA and CO_2 concentrations and loadings in 2B4D and $(2B4D)_L$ at different loadings

Solvent		BDA	DEEA	CO_2	CO_2 loading
		(mol/kg)	(mol/kg)	(mol/kg)	(mol/mol amine)
2B4D	Upper phase	0.115	7.265	0.315	0.043
	Lower phase rich	2.233	2.400	3.291	0.710
	Lower phase lean	2.477	2.663	1.050	0.204
	2B4D lean	2.200	3.906	0.943	0.154
$(2B4D)_L$	Fresh	2.607	2.806	/	/
	Rich	2.268	2.441	3.398	0.722
	Lean	2.490	2.679	1.076	0.208

Figure 3 shows the cyclic loadings and cyclic capacities of the 2B4D lower phase and $(2B4D)_L$, indicating that the cyclic capacity and cyclic loading of 2B4D and $(2B4D)_L$ are very similar. Therefore, $(2B4D)_L$ differs little from the lower phase of 2B4D in terms of the cyclic capacity and cyclic loading.

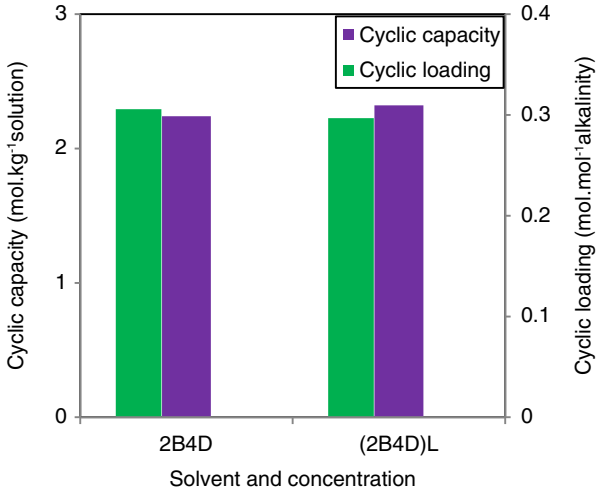

Figure 3

Comparison of cyclic capacities and cyclic loadings of 2B4D and $(2B4D)_L$.

3.3 Comparison of Absorption Rate

The influence of the saturator added to the WWC system was investigated by titrating DEEA concentration against 0.2 N H_2SO_4 using a *Metrohm* 809 Titrando auto titrator before and after the WWC tests of aqueous DEEA solution. The results listed in Table 2 confirm that the addition of the saturator effectively balanced the water in the system.

The parameters α and β in Equation (13) were determined with SO_2 absorption into 0.1 M NaOH solution to determine the gas side mass transfer coefficient k_g. The results are listed in Table 3 with a correlation in Figure 4.

Therefore, the correlated equation for the gas side mass transfer coefficient is Equation (14):

$$Sh = 6.7097(Re \times Sc \times d_h/h)^{0.5036} \qquad (14)$$

The CO_2 absorption rates for 2B4D and $(2B4D)_L$ were measured with WWC system at 298.15, 313.15

TABLE 2

Titration results of DEEA concentrations before and after the WWC experiment

Sample	Sample amount (g)	H_2SO_4 (mL)	DEEA concentration (mol.kg^{-1})
Before WWC	0.8880	17.8741	4.0538
After WWC	0.8531	17.1017	4.0374

TABLE 3

Correlation of gas-side mass transfer coefficient k_g fitted with SO_2 absorption into 0.1 M NaOH solution

Total flow rate	P	$k_g \times 10^{10}$	$Re \times Sc \times d_h/h$	Sh
(L/min)	(MPa)	(mol/Pa·cm^2·s)		
5.84	0.13	8.38	43.39	44.70
6.11	0.15	7.47	45.38	45.14
8.13	0.17	7.89	60.35	54.16
8.26	0.14	9.07	61.35	52.16
3.56	0.16	5.10	26.43	32.74
3.69	0.16	5.56	27.42	36.36
3.96	0.17	5.52	29.42	38.15
9.88	0.17	8.67	73.32	59.19
1.54	0.17	3.39	11.46	23.17

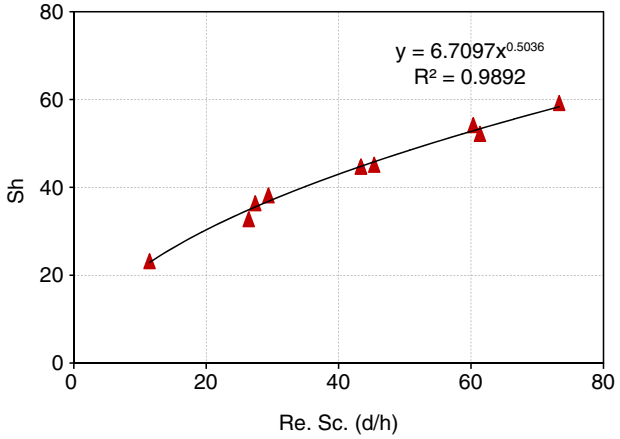

Figure 4

Correlation curve of gas-side mass transfer coefficient k_g fitted by SO_2 absorption into 0.1 M NaOH solution.

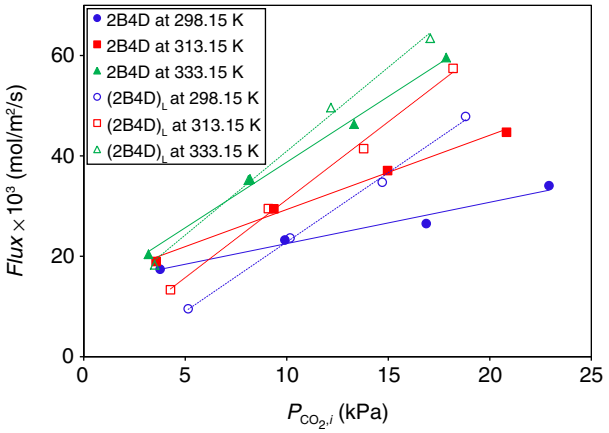

Figure 5

Flux-$P_{CO_2,i}$ relationship of fresh 2B4D and $(2B4D)_L$ solutions.

and 333.15 K with the CO_2 pressure of 3-25 kPa at loadings of 0 (fresh solution), half lean loading and lean loading, as presented in Tables 4 and 5.

The Flux of 2B4D and $(2B4D)_L$ at 0 loading, half lean loading and lean loading are compared in Figures 5 to 7. Figure 5 shows that the fresh 2B4D solution reacted faster than $(2B4D)_L$ with $P_{CO_2,i}$ lower than 8 kPa, while the absorption rate of the fresh $(2B4D)_L$ solution was higher than that of fresh 2B4D solution with $P_{CO_2,i}$ higher than 10 kPa. Figure 6 reveals that at half lean loading, the absorption rate of $(2B4D)_L$ was higher than that of 2B4D for $P_{CO_2,i}$ between 5 and 25 kPa. Figure 7 shows that at the lean loading, $(2B4D)_L$ reacted faster than 2B4D. For example, the mass flux of $(2B4D)_L$ at lean loading and 313.15 K was 37% higher than that of 2B4D. Comparing the 3 figures, at 313 K and $P_{CO_2,i}$ = 15 kPa, the mass flux of fresh $(2B4D)_L$ solution was twice more than that at lean loading and the mass flux of fresh 2B4D was 2.2 times more than that at lean loading.

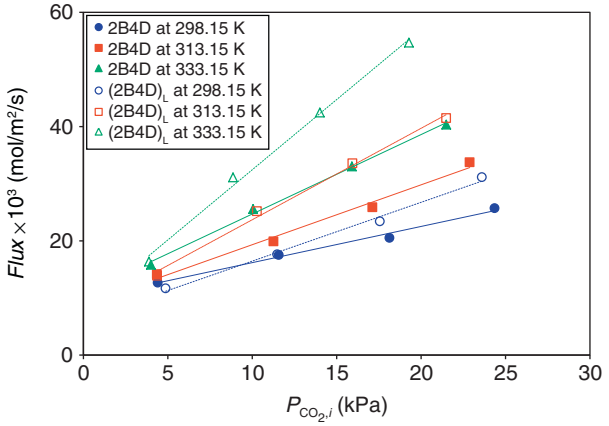

Figure 6

Flux-$P_{CO_2,i}$ relationship of 2B4D and $(2B4D)_L$ solution at their half lean loadings.

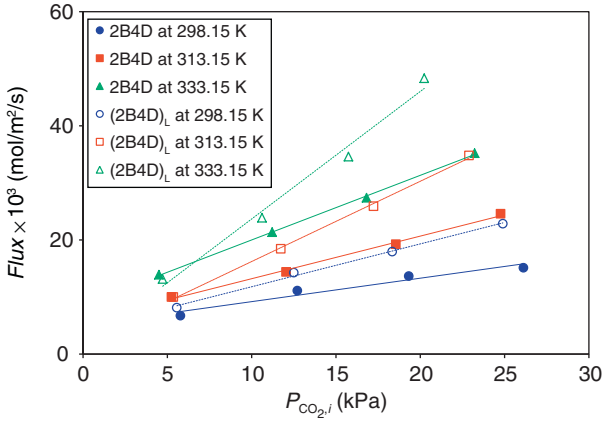

Figure 7

Flux-$P_{CO_2,i}$ relationship of 2B4D and $(2B4D)_L$ solution at their lean loadings.

3.4 Comparison of the Reaction Products

As for the reaction products, our previous research has identified the carbon numbers, as shown in Table 6 (Xu *et al.*, 2013c). The peaks positions of the fresh 2B4D solution NMR spectrum agreed well with those in the literature (Balaban *et al.*, 1985; Parker *et al.*, 2011). Comparison of the NMR data and the titration results showed that the NMR error was less than 8%. (Xu *et al.*, 2013c)

TABLE 4
Kinetic parameters of CO_2 absorption into 2B4D solutions at 298.15, 313.15 and 333.15 K

Solvent	T (K)	$Flux \times 10^3$ (mol/m^2/s)	$P_{CO_2,b}$ (kPa)	$k_g \times 10^6$ (mol/Pa/m^2/s)	$P_{CO_2,i}$ (kPa)
2B4D fresh	298.15	17.41	5.80	8.55	3.76
		23.24	12.67	8.42	9.91
		26.51	20.02	8.41	16.87
		34.06	26.98	8.39	22.92
	313.15	18.96	5.85	8.30	3.56
		29.46	12.93	8.27	9.37
		37.07	19.46	8.25	14.97
		44.71	26.25	8.23	20.83
	333.15	20.41	5.68	8.17	3.19
		35.39	12.54	8.13	8.19
		46.32	19.07	8.05	13.32
		59.59	25.23	8.08	17.85
2B4D half lean loading	298.15	12.68	5.90	8.50	4.41
		17.53	13.65	8.43	11.57
		20.52	20.58	8.36	18.13
		25.71	27.43	8.35	24.35
	313.15	14.15	6.06	8.31	4.35
		19.89	13.65	8.29	11.26
		25.86	20.26	8.22	17.11
		33.74	26.99	8.21	22.88
	333.15	15.80	5.92	8.24	4.00
		25.55	13.20	8.10	10.05
		33.01	19.99	8.09	15.90
		40.34	26.49	8.07	21.49
2B4D lean loading	298.15	6.71	6.57	8.46	5.78
		11.11	14.02	8.50	12.71
		13.67	20.93	8.50	19.32
		15.12	27.92	8.44	26.12
	313.15	10.00	6.44	8.37	5.25
		14.39	13.77	8.36	12.05
		19.24	20.87	8.30	18.55
		24.59	27.74	8.28	24.77
	333.15	13.90	6.20	8.19	4.50
		21.36	13.85	8.11	11.22
		27.40	20.15	8.21	16.81
		35.21	27.61	8.03	23.23

TABLE 5
Kinetic parameters of CO_2 absorption into $(2B4D)_L$ solutions at 298.15, 313.15 and 333.15 K

Solvent	T (K)	$Flux \times 10^3$ (mol/m^2/s)	$P_{CO_2,b}$ (kPa)	$k_g \times 10^6$ (mol/Pa/m^2/s)	$P_{CO_2,i}$ (kPa)
$(2B4D)_L$ fresh	298.15	9.55	6.26	8.57	5.14
		23.65	12.92	8.59	10.16
		34.75	18.73	8.62	14.70
		47.85	24.34	8.65	18.81
	313.15	13.33	5.85	8.42	4.27
		29.51	12.64	8.33	9.10
		41.44	18.82	8.24	13.79
		57.43	25.19	8.20	18.19
	333.15	18.30	5.74	8.12	3.49
		35.16	12.46	8.08	8.11
		49.63	18.30	8.10	12.17
		63.44	24.93	8.07	17.07
$(2B4D)_L$ half lean loading	298.15	11.68	6.26	8.39	4.87
		17.63	13.60	8.32	11.48
		23.40	20.36	8.36	17.56
		31.14	27.33	8.34	23.60
	313.15	13.88	6.05	8.25	4.36
		25.17	13.36	8.17	10.28
		33.56	20.02	8.21	15.93
		41.47	26.55	8.19	21.48
	333.15	16.36	5.87	8.24	3.88
		31.10	12.71	8.09	8.86
		42.45	19.27	8.06	14.00
		54.68	26.13	7.98	19.28
$(2B4D)_L$ lean loading	298.15	8.13	6.53	8.45	5.56
		14.26	14.19	8.44	12.50
		17.95	20.47	8.43	18.34
		22.84	27.61	8.42	24.90
	313.15	10.00	6.56	8.32	5.36
		18.45	13.95	8.30	11.73
		25.90	20.36	8.28	17.23
		34.79	27.11	8.26	22.90
	333.15	13.16	6.34	8.13	4.72
		23.89	13.60	8.00	10.62
		34.59	20.05	8.03	15.74
		48.34	26.24	8.05	20.24

TABLE 6
Identification of carbon atoms in NMR spectrum (Xu *et al.*, 2013c)

Component	Structure and identification
DEEA/DEEAH$^+$	
BDA/BDAH$^+$/BDAH$_2^{2+}$	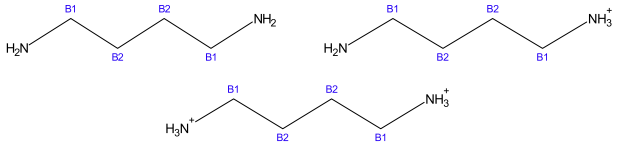
BDACOO$^-$/HBDACOO	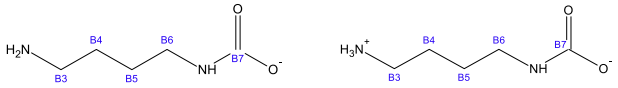
BDA(COO$^-$)$_2$	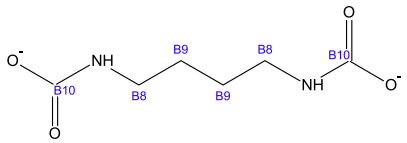
CO_3^{2-}/HCO_3^-	

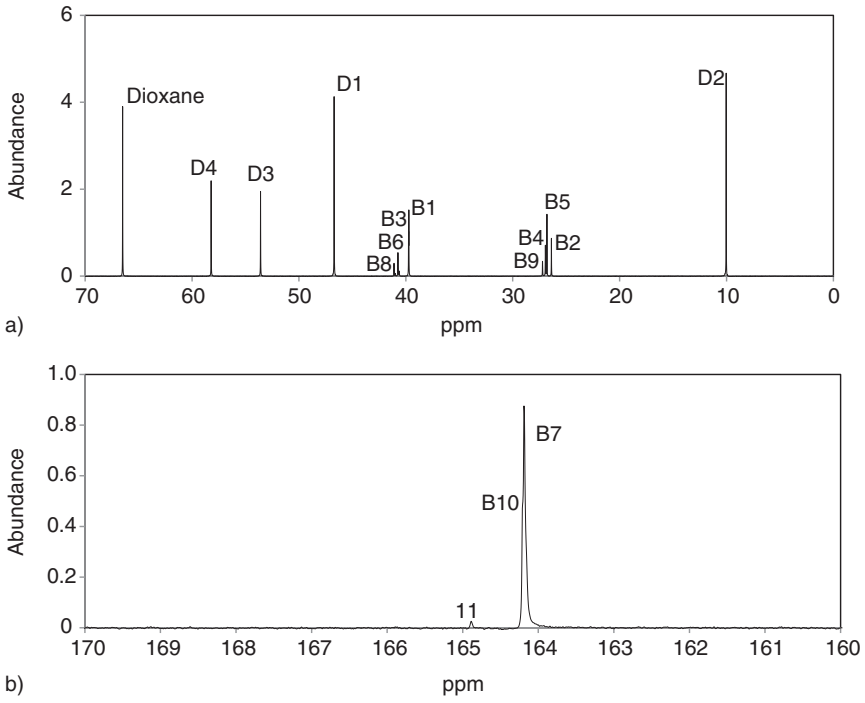

Figure 8

NMR spectrum of (2B4D)$_L$ at the loading of 0.361 mol/mol amine. a) Up field part spectrum; b) low field part spectrum.

TABLE 7
Comparison of the CO_2 concentrations measured by NMR and titration in $(2B4D)_L$

Loading (mol/mol amine)	NMR results				CO_2 by titration (mol/kg)	Error (%)
	BDACOO (mol/kg)	$BDA(COO)_2$ (mol/kg)	CO_3^{2-}/HCO_3^- (mol/kg)	CO_2 by NMR (mol/kg)		
0.113	0.430	0.000	0.147	0.577	0.543	5.83
0.219	0.803	0.109	0.099	1.119	1.028	8.08
0.361	1.051	0.293	0.125	1.762	1.641	6.85
0.532	1.282	0.614	0.049	2.558	2.341	8.49
0.735	1.095	0.815	0.530	3.256	3.112	4.42

In this work, the quantitative NMR spectrum of $(2B4D)_L$ at five various loadings were acquired. The loadings of all solutions were controlled by the amount of CO_2 bubbled into the solution and verified by titration against 0.2 N H_2SO_4. The five loadings were 0.113, 0.219, 0.361, 0.532 and the rich loading 0.735 mol CO_2/mol amine.

The NMR results of the solution with the 0.361 mol/mol loading are shown in Figure 8 as an example. Referring to the NMR spectrum for fresh 2B4D solution (Xu *et al.*, 2013c), the BDA and DEEA positions can be easily recognized and the positions of D1, D2, D3, D4, B1 and B2 can be identified in the figure. B3, B4, B5 and B6 represent BDA carbamate, the peak areas of which must be equal and close to those of B1 and B2, so they can also be identified in the spectrum. Then, the remaining peaks are B8 and B9 in Figure 8a. The peaks in Figure 8b are B7, B10 and 11. As previous researchers have pointed out, due to the fast proton exchange with water, it is not possible to distinguish signals of amine from protonated amine, or carbonate from bicarbonate. Thus, the position of these peaks in the spectra are the average of the chemical shift of amine and proton amine, or carbonate and bicarbonate (Jakobsen *et al.*, 2005, 2008; Hartono *et al.*, 2007). Thus in the following tables and figure legends of all species represent species and their protonated forms. For example, BDA represents the sum of BDA, $BDAH^+$ and $BDAH_2^{2+}$.

The NMR results in this paper are compared with the titration results to verify its accuracy, as shown in Table 7. The CO_2 concentration measured by the NMR result is the sum of BDA carbamate, bicarbamate and carbonate/bicarbonate. The difference between the NMR and titration results indicates the accuracy of NMR results of this work.

The concentrations of the various $(2B4D)_L$ species at different loadings are shown in Figure 9. It is obvious

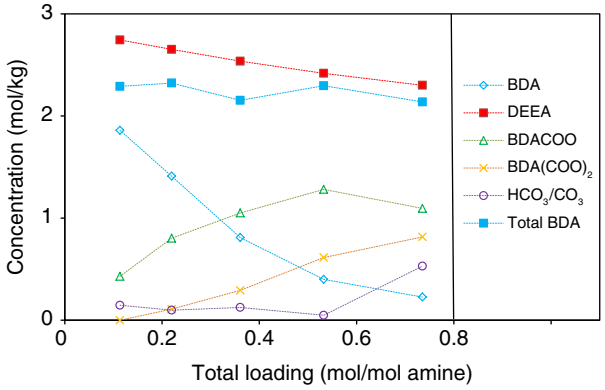

Figure 9
Concentrations of $(2B4D)_L$ species at various loadings.

that BDA concentration decreased from 1.859 mol/kg solution at the loading of 0.113 mol/mol to 0.206 mol/kg at the rich loading of 0.735 mol/mol. The BDA carbamate concentration first increased and then decreased slightly after the loading of 0.532 mol/mol, possibly due to the formation of bicarbamate. BDA bicarbamate kept increasing with increased loading. BDA bicarbamate concentration was higher than the BDA concentration at high loadings. The carbonate/bicarbonate concentration increased sharply after the loading of 0.532 mol/mol as a result of DEEA reaction with CO_2.

Figure 10 presents the species mole fraction variations of BDA with the increased loading. Since the total BDA concentration did not vary much during the absorption, the tendency of mole fractions is similar to the variations in Figure 9. Figure 10 also demonstrates that at higher loadings, the mole fraction of BDA bicarbamate was relatively high. At rich loading, the mole fractions of BDA, $BDACOO^-$ and $BDA(COO)_2^{2-}$ were 10.62%, 51.23% and 38.15%, respectively.

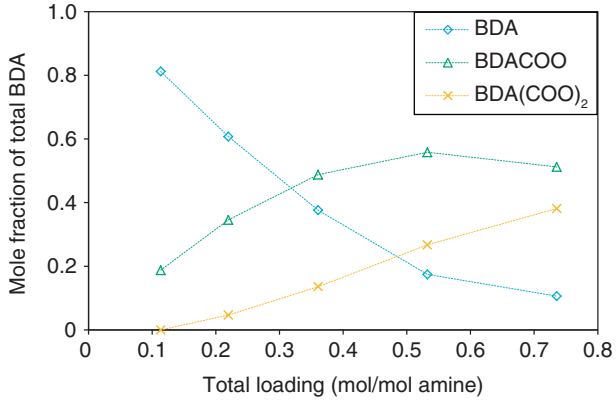

Figure 10

Mole fractions of BDA species in $(2B4D)_L$ at various loadings.

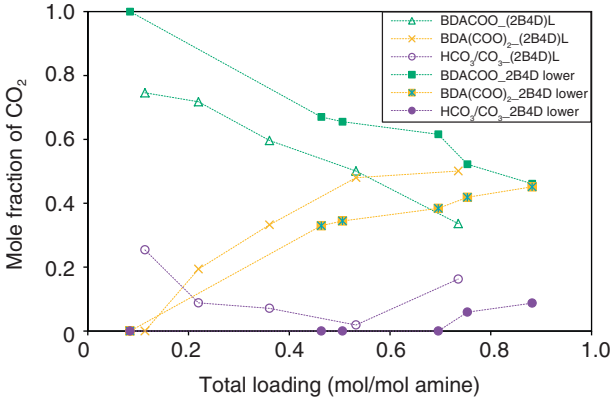

Figure 11

Comparison of CO_2 distribution in terms of BDACOO, $BDA(COO)_2$ and CO_3^{2-}/HCO_3^- between 2B4D and $(2B4D)_L$ at different loadings.

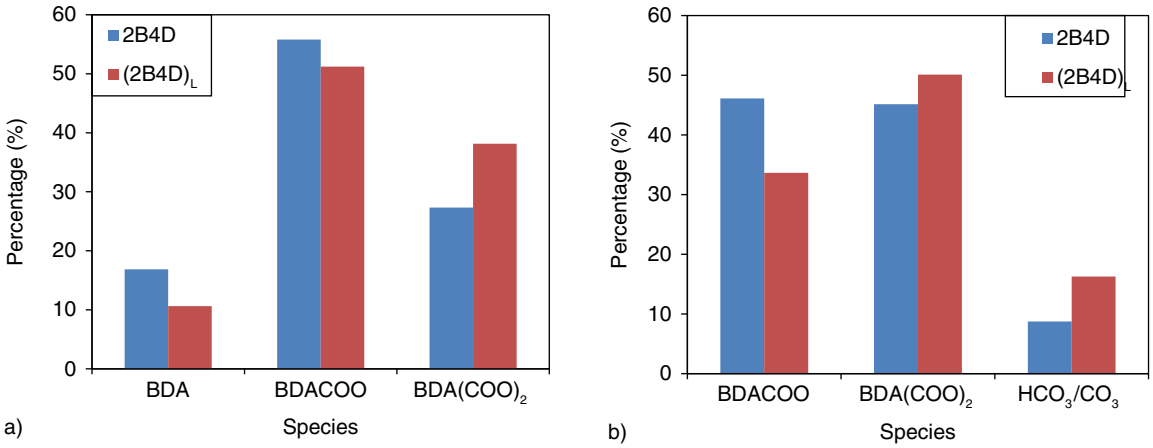

Figure 12

BDA and CO_2 reaction products distributions in 2B4D and $(2B4D)_L$ at the rich loading. a) BDA distribution; b) CO_2 distribution.

Figure 11 illustrates the distribution of CO_2 in terms of $BDACOO^-$, $BDA(COO)_2^{2-}$ and CO_3^{2-}/HCO_3^-. The current NMR spectrum, unfortunately, had no peaks around 125 ppm, which would indicate free CO_2. As the results of Jokobsen *et al.* (2005) and Suda *et al.* (1996) proved that the free CO_2 was less than 5% of its total amount in the solution, the free CO_2 in the solution was neglected in this work. Given that BDA bicarbamate has two carbon atoms, its mole fraction in the figure is twice as its actual fraction. Figure 11 shows that at the beginning, the CO_2 formed BDA carbamate, while the BDA carbamate fraction decreased and bicarbamate increased with increasing CO_2 loading. At the rich loading, CO_2 in the solution was distributed as 33.64% carbamate, 50.10% bicarbamate and 16.26% carbonate/bicarbonate.

Figure 11 also compares the CO_2 distribution between 2B4D lower phase and $(2B4D)_L$ at different loadings. The CO_2 distribution in 2B4D lower phase can be referred to Xu *et al.* (2013c). It shows that in $(2B4D)_L$ solution, the mole fraction of CO_2 existed in terms of carbamate was more than that in 2B4D lower phase, while the mole fractions of CO_2 in terms of bicarbamate and carbonate/bicarbonate were slightly higher than those in 2B4D lower phase.

The reaction products and the BDA and CO_2 distributions in 2B4D and $(2B4D)_L$ at the rich loading are compared in Figure 12. Figure 12a shows that the $(2B4D)_L$

reaction products had more BDA bicarbamate than the 2B4D products, with less BDA and less BDA carbamate. Figure 12b demonstrates that the CO_2 reaction products of $(2B4D)_L$ had twice as much carbonate/bicarbonate as 2B4D and less BDA carbamate. The reason for more BDA bicarbamate of $(2B4D)_L$ is that the BDA concentration in $(2B4D)_L$ was almost constant during absorption, while the equivalent BDA concentration (including BDA carbamate and bicarbamate) in the 2B4D lower phase kept decreasing while approaching the rich loading. The BDA concentration of 2B4D lower phase at different loadings can be referred to Xu *et al.* (2013c).

CONCLUSIONS

The present study identifies the $(2B4D)_L$ composition with 2.607 mol/kg BDA and 2.806 mol/kg DEEA. The cyclic capacity and cyclic loading of $(2B4D)_L$ are almost the same as those of 2B4D. For reaction conditions of 298.15, 313.15 and 333.15 K and CO_2 pressure of 3-25 kPa, the absorption rates of fresh $(2B4D)_L$ solution, $(2B4D)_L$ solutions at half lean loading and lean loading are higher than those of fresh 2B4D solution, and 2B4D solutions at half lean loading and lean loading, respectively, except for the fresh solutions at CO_2 pressure lower than 10 kPa.

NMR measurements of the reaction products of $(2B4D)_L$ show that in $(2B4D)_L$ solution, the BDA bicarbamate concentration increases with increasing CO_2 loading, while the BDA carbamate concentration decreases a little at loadings greater than 0.532 mol/mol. The reaction products of $(2B4D)_L$ have more BDA bicarbamate, less BDA and less BDA carbamate than 2B4D. The CO_2 reaction products of $(2B4D)_L$ have twice as much carbonate/bicarbonate as with 2B4D and less BDA carbamate. Further study on the performance of $(2B4D)_L$ is necessary.

ACKNOWLEDGMENTS

Financial support from the Chinese MOST project "Key Technology Research and Development on Advanced Coal Conversion and Power Generation" (2010DFA72730) is greatly appreciated.

REFERENCES

Aronu U.E., Hoff K.A., Svendsen H.F. (2011) CO_2 capture solvent selection by combined absorption-desorption analysis, *Chem. Eng. Res. Des.* **89**, 1197-1203.

Balaban A.T., Dinculescu A., Elguero J., Faure R. (1985) Carbon-13 NMR studies of primary amines and their corresponding 2,4,6-trimethyl-pyridinium salts, *Magn. Reson. Chem.* **23**, 553-558.

Bishnoi S., Rochelle G.T. (2002) Absorption of carbon dioxide in aqueous piperazine/methyldiethanolamine, *AIChE J.* **48**, 2788-2799.

Bruder P., Svendsen H.F. (2011) Solvent comparison for post combustion CO_2 capture, *1st Post Combustion Capture Conference*, 17-19 May, Abu Dhabi, Kingdom of Saudi Arabia.

Derks P.W.J., Dijkstra H.B.S. (2005) Solubility of carbon dioxide in aqueous piperazine solutions, *AIChE J.* **51**, 2311-2327.

Hartono A., da Silva E.F., Grasdalen H., Svendsen H.F. (2007) Qualitative determination of species in DETA-H_2O-CO_2 system using ^{13}C NMR spectra, *Ind. Eng. Chem. Res.* **46**, 249-254.

Hilliard M.D. (2008) A predictive thermodynamic model for an aqueous blends of potassium carbonate, piperazine, and monoethanolamine for carbon dioxide capture from flue gas, *PhD Thesis*, University of Texas, Austin.

Hu L. (2009) Phase transitional absorption method, *United States Patent*, 7541001.

Jakobsen J.P., Krane J., Svendsen H.F. (2005) Liquid-phase composition determination in CO_2-H_2O-alkanolamine system: an NMR study, *Ind. Eng. Chem. Res.* **44**, 9894-9903.

Jakobsen J.P., da Silva E.F., Krane J., Svendsen H.F. (2008) NMR study and quantum mechanical calculations on the 2-[(2-aminoethyl) amino]- ethianol- H_2O- CO_2 system, *J. Magn. Reson.* **191**, 304-314.

Liu J., Wang S., Zhao B., Tong H., Chen C. (2009) Absorption of carbon dioxide in aqueous ammonia, *Energy Procedia* **1**, 933-940.

Liu J., Wang S., Qi G., Zhao B., Chen C. (2011) Kinetics and mass transfer of carbon dioxide absorption into aqueous ammonia, *Energy Procedia* **4**, 525-532.

Liu J., Wang S., Zhao B., Chen C. (2012) Study on mass transfer and kinetics of CO_2 absorption into aqueous ammonia and piperazine blended solutions, *Chem. Eng. Sci.* **75**, 298-308.

Pacheco M.A. (1998) Mass transfer, kinetics and rate-based modeling of reactive absorption, *PhD Thesis*, University of Texas, Austin.

Parker E., Leconte N., Godet T., Belmont P. (2011) Solver-catalyzed furoquinolines synthesis: from nitrogen effects to the use of silver imidazolate polymer as a new and robust silver catalyst, *Chem. Commun.* **47**, 343-345.

Raynal L., Alix P., Bouillon P.A., Gomez A., de Nailly M.F., Jacquin M., Kittel J., di Lella A., Mougin P., Trapy J. (2011) The DMX^{TM} process: An original solution for lowering the cost of post-combustion carbon capture, *Energy Procedia* **4**, 779-786.

Rinker E.B., Ashour S.S. (2000) Absorption of carbon dioxide into aqueous blends of diethanolamine and methyldiethanolamine, *Ind. Eng. Chem. Res.* **39**, 4346-4356.

Rochelle G.T. (2009) Amine scrubbing for CO_2 capture, *Science* **325**, 1652-1654.

Rojey A., Cadours R., Carrette P.L., Boucot P. (2009) Method of deacidizing a gas by means of an absorbent solution with fractionated regeneration through heating, *United States Patent*. Pub. No.: US 2009/0199709 A1.

Suda T., Iwaki T., Mimura T. (1996) Facile determination of dissolved species in CO_2-amine-H_2O system by NMR spectroscopy, *Chem. Lett.* **9**, 777-778.

Svendsen H.F., Hessen E.T., Mejdell T. (2011) Carbon dioxide capture by absorption, challenges and possibilities, *Chem. Eng. J.* **171**, 718-724.

Tan Y.H. (2010) Study of CO_2-absorption into thermomorphic lipophilic amine solvents, *PhD Thesis*, University of Dortmund, Germany.

Xu Z., Wang S., Liu J., Chen C. (2012a) Solvents with low critical solution temperature for CO_2 capture, *Energy Procedia* **23**, 64-71.

Xu Z., Wang S., Zhao B., Chen C. (2012b) Study on potential biphasic solvents: absorption capacity, CO_2 loading and reaction rate, *11th International Conference on Greenhouse Gas Technologies*, 18-22 Nov., Kyoto, Japan.

Xu Z., Wang S., Chen C. (2013a) Experimental study of CO_2 absorption by biphasic solvents, *J. Tsinghua University (Science and Technology)* **53**, 3, 336-341.

Xu Z.C., Wang S.J., Chen C.H. (2013b) Experimental Study of CO_2 absorption by MAPA, DEEA, BDA and BDA/DEEA mixtures, *J. Combust. Sci. Technol.* **19**, 2, 103-108.

Xu Z., Wang S., Chen C. (2013c) CO_2 absorption by biphasic solvents: mixtures of 1,4-Butanediamine and 2-(Diethylamino)-ethanol, *Int. J. Greenhouse Gas Control* **16**, 107-115.

Zhang J., Agar D.W., Zhang X., Geuzebroek F. (2011) CO_2 absorption in biphasic solvents with enhanced low temperature solvent regeneration, *Energy Procedia* **4**, 67-74.

Zhang X. (2007) Studies on multiphase CO_2 capture system, *PhD Thesis*, University of Dortmund, Germany.

Manuscript accepted in May 2013
Published online in November 2013